Caucasian Journal of Science
ISSN: 2148-6840
https://doi.org/ 10.48138/cjo.1205712
Year: 2022
Volume: 9 Issue: 2

Determination of Intermolecular Interactions of Nicotinamide Liganded Complexes of Co(II), Cu(II), Ni(II) and Zn(II) 4-Formylbenzoates by Hirshfeld Surface Analysis and Investigation of Interaction Energies

Mustafa SERTÇELİK[1]

Makalenin Alanı: Chemistry

Makale Bilgileri

Geliş Tarihi
16.11.2022
Kabul Tarihi
22.12.2022
Anahtar Kelimeler
CrystalExplorer
Hirshfeld yüzey analizi
Metal kompleks
4-Formilbenzoat
Nikotinamid

Öz

CrystalExplorer programı teorik kimya alanında son yıllarda sıklıkla kullanılan ve popülaritesi artan bir programıdır. Öncelikli olarak bu programda moleküllerin Hirshfeld yüzey analizi yapılabilmektedir. Hirshfeld yüzey analizi sayesinde moleküller arası etkileşimler ve bu etkileşimlerin kristal yüzeye katkıları belirlenebilmektedir. Bu çalışmada Co(II), Cu(II), Ni(II) ve Zn(II) 4-formilbenzoatın nikotinamid komplekslerinin Hirshfeld yüzey analizleri ve enerji çerçeveleri incelenmiştir. Tüm kompleksler için dnorm indeksi, şekil indeksi kavislilik indeksi ve 2B parmak izi grafikleri incelenmiştir. Bunun yanında CE-B3LYP/6-31G (d,p) ve CEHF/3-21G enerji modelleri kullanılarak komplekslerin moleküller arası etkileşim enerjileri hesaplanmıştır. Tüm bunların neticesinde isoyapılı olan dört komplekste en önemli etkileşimin H...H etkileşimleri olduğu görüldü. Hirshfeld yüzey analizi ve enerji çerçevelerine göre O-H···O ve N-H···O hidrojen bağları ve π···π istifleme ve C–H···π etkileşim enerjileri kristal yapıdaki en önemli etkileşim türleri olarak görülmektedir.

Article Info

Received
16.11.2022
Accepted
22.12.2022
Keywords
CrystalExplorer
Hirshfeld surface analysis
Metal complex
4-Formylbenzoate
Nicotinamide

Abstract

CrystalExplorer program is a program that has been used frequently in the field of theoretical chemistry in recent years and its popularity has increased. First of all, Hirshfeld surface analysis of molecules can be done in this program. Thanks to Hirshfeld surface analysis, intermolecular interactions and their contributions to the crystal surface can be determined. In this study, Hirshfeld surface analyzes and energy frameworks of nicotinamide complexes of Co(II), Cu(II), Ni(II) and Zn(II) 4-formylbenzoate were investigated. Dnorm index, shape index, curvature index and 2D fingerprint graphs were examined for all complexes. In addition, the intermolecular interaction energies of the complexes were calculated using the CE-B3LYP/6-31G (d,p) and CEHF/3-21G energy models. As a result of all these, it was seen that the most important interaction in the four isostructured complexes was H...H interactions.
According to Hirshfeld surface analysis and energy frameworks, O-H···O and N-H···O hydrogen bonds and π···π stacking and C–H··π interaction energies are seen as the most important interaction types in the crystal structure.

INTRODUCTION

The structural, physical and biological properties of materials produced in materials science are extremely important in terms of the usage area of that material(Sertçelik et al., 2012; Huseynova et al., 2019; Sertçelİk et al., 2018; Huseynova et al., 2020; Sertcelik &

[1] Kafkas Üniversitesi, Mühendislik Mimarlık Fakültesi-Kars; e-mail: mustafasertcelik@gmail.com; ORCID: 0000-0001-7919-7907 (Corresponding author)

Durman, 2020; Sugeçti & Büyükgüzel, 2022). Experimental research on these is a very costly and time-consuming task. Therefore, the importance of theoretical chemistry is increasing day by day. Thanks to theoretical chemistry, we can obtain theoretical information before carrying out the studies experimentally (Irak & Beytur, 2019; Kotan et al., 2020; Koç et al., 2020). Making the theoretical calculations before the experiments is a great gain for the scientists because both the raw material consumption is reduced and there is no loss of time. CrystalExplorer program is a frequently used program among theoretical calculation programs (Huseynova, 2021; Kirste, 2016; Omoregie et al., 2022; Sertçelik, 2021). With this program, the Hirshfeld surface analysis of a molecule can be determined. Hirshfeld surface analysis allows us to see the interactions of intermolecular contact types in a crystal structure. It allows us to have information about the interactions between molecules in the crystal structure. With this method, we can determine the similarities and differences between crystal structures and the percentage of interaction between all atoms of molecules.

In this study, the intermolecular interactions of nicotinamide liganded complexes of Co(II), Cu(II), Ni(II) and Zn(II) 4-formylbenzoate were calculated. Separately, dnorm map, shape index, curvature map, 2D fingerprint plots and crystalline fragment patches were determined. For the energy framework analysis of the complex, electrostatic energy, polarization energy, dispersion energy, exchange-repulsion energy and total intermolecular energy were calculated using the model CE-HF/3-21G and CE-B3LYP/6-31G (d,p) as energy.

MATERIALS AND METHOD

Hirshfeld surface analysis was used to investigate the visualization of the intermolecular interactions of complexes Diaquabis (4-formylbenzoato-κO^1) bis (nicotinamide-κN^1) cobalt(II)(Sertçelik et al., 2012c), Diaquabis (4-formylbenzoato-κO^1) bis (nicotinamide-κN^1) copper(II)(Sertçelik et al., 2012a), Diaquabis (4-formylbenzoato-κO^1) bis (nicotinamide-κN^1) nickel(II)(Sertçelik et al., 2012b) and Diaquabis (4-formylbenzoato-κO^1) bis (nicotinamide-κN^1) zinc(II)(Sertçelik et al., 2012d) which we have previously synthesized and characterized.

Intermolecular interactions of the complex were analyzed using the crystallographic information file (CIF) of the compounds with the help of CrystalExplorer 17.5 program(Turner et al., 2017). As a result of these analyzes, Hirshfeld surface, dnorm and curvature maps and shape index and 2D fingerprint graphs were obtained. To gain greater accuracy about

molecular interactions, the Tonto quantum chemistry package was utilized for energy framework analysis(Jayatilaka et al., 2005; McKinnon et al., 2007; Spackman et al., 2008; Spackman & Jayatilaka, 2009). Intermolecular interaction energies of the complexes were calculated using the CE-HF/3-21G and CE-B3LYP/6-31G (d,p) energy models in CrystalExplorer program.

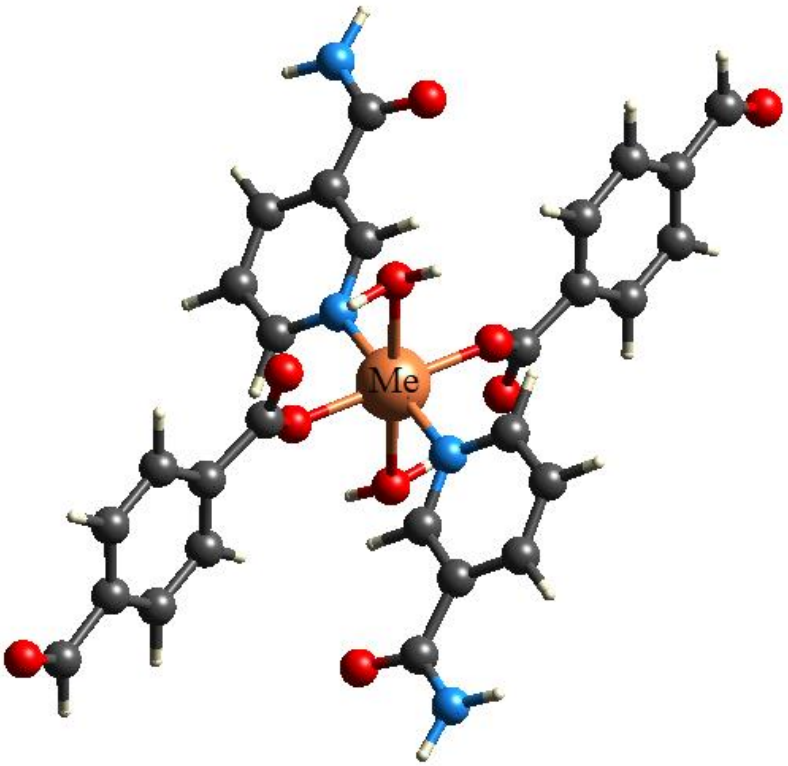

Figure 1. Crystal structure of complexes

RESULTS AND DISCUSSION

Hirshfeld Surface Analysis

Hirshfeld surface (HS) analysis was performed using Crystal Explorer 17.5 to visualize the intermolecular interactions of the complexes. The white surface in the HS plotted over dnorm (Figure 2a-5a) denotes contacts with distances equal to the sum of van der Waals radii, whereas the red and blue colors denote connections with distances that are closer together or farther apart (distinct contact), respectively(Venkatesan et al., 2016). Their respective functions as donors and/or acceptors are indicated by the vivid red patches that appear. It shows π ··· π interactions with the presence of adjacent red and blue triangles in the shape

index of the HS. If there is no adjacent red and/or blue triangle, there is no π ·· π interaction. Figure 2b-5b clearly shows the red blue triangles, which are evidence of π ·· π interactions. The benzene and pyridine ring ligands are positioned in rather large green planes. A crystal system's curvedness mapping provides insight into the planarity of complexes that give rise to the π ·· π interactions between the benzene and pyridine rings (Figure 2c-5c) (Spackman et al., 2008).

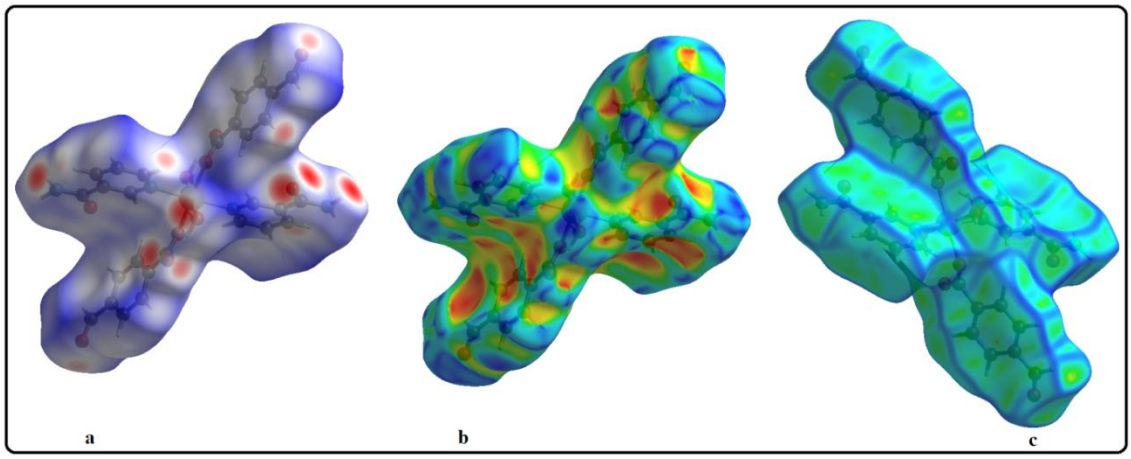

Figure 2. Dnorm map, shape index and curvature map of Complex I.

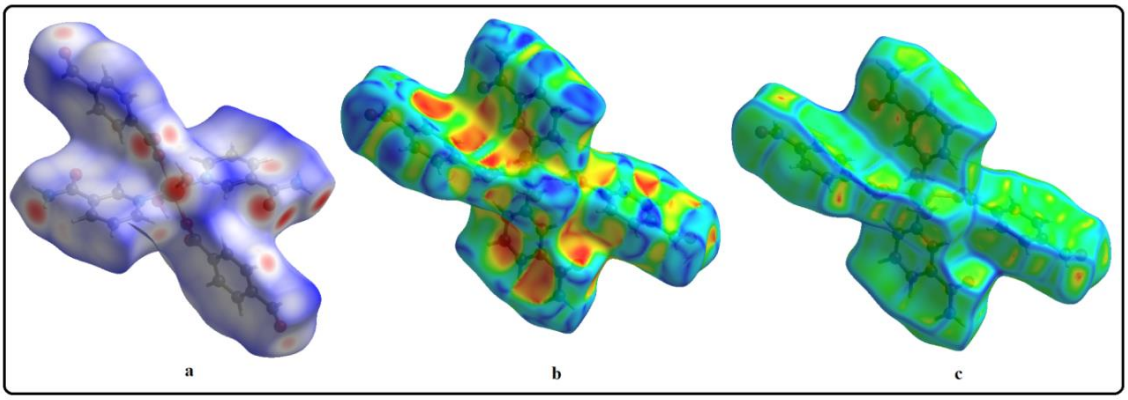

Figure 3. Dnorm map, shape index and curvature map of Complex II.

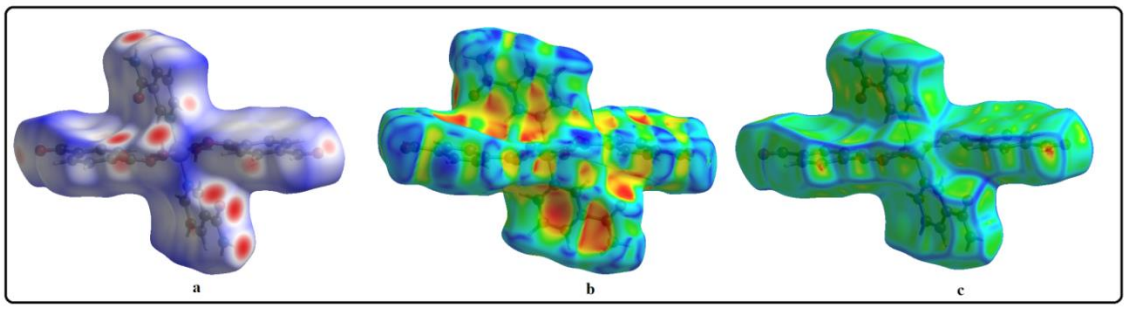

Figure 4. Dnorm map, shape index and curvature map of Complex III.

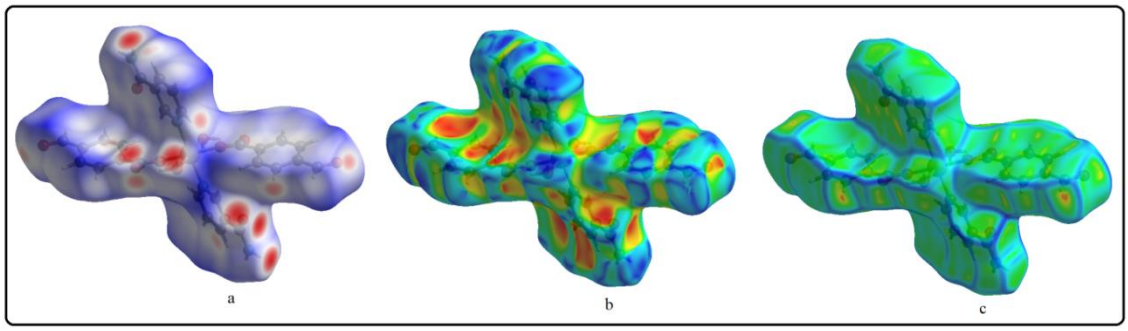

Figure 5. Dnorm map, shape index and curvature map of Complex IV.

2D fingerprint plots for all examined complexes are given in Figure 6-9. All complexes are isostructure. The intermolecular interactions that contribute to the crystal packing of these four complexes are nearly identical (Table 6-9). In the 2D fingerprint graphs of all complexes, the most dominant interaction is the H···H interaction (Fig. 6b-9b). Their contribution to the crystal surface is 31.10%, 30.80%, 31.30% and 31.20%, respectively (Figure 10). The H···H interactions dominate because of the abundance of hydrogen on the molecular surface. The second dominant interaction is the O···H/H···O interaction (Figure 6c-9c). Here, the interaction percentages were calculated as 29.80, 30.00, 29.60 and 29.80, respectively (Figure 10). It is seen that the third highest interaction is the interactions originating from C···H/C···H bonds (Figure 6d-9d). The interaction percentages are 25.80, 26.80, 25.90 and 25.80, respectively (Figure 10). The presence of high rates of H···H, H...O/O...H and H···C/C···H interactions in all of the complexes indicates that van der Waals interactions and hydrogen bonding play a major role in crystal packing. The percentages of all interactions in the complexes are given in Table 10.

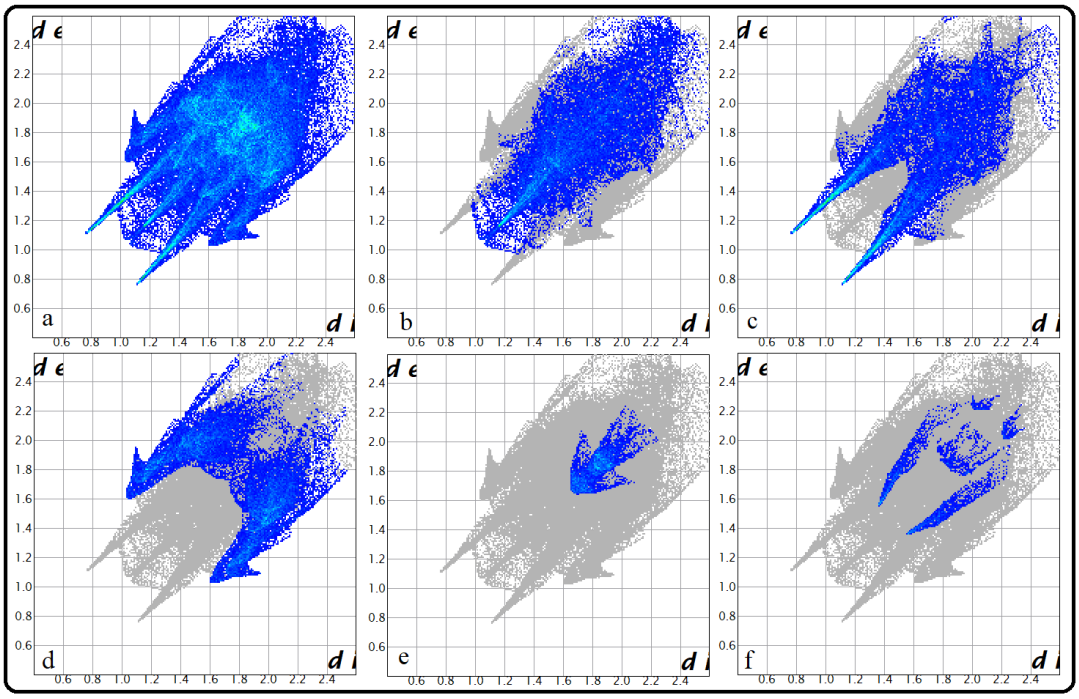

Şekil 6. The full two-dimensional fingerprint plots for the complex I, showing (a) all atoms interactions and delineated into (b) H···H, (c) H···O/O···H, (d) H···C/C···H, (e) C···C and (f) C···O/O···C interactions.

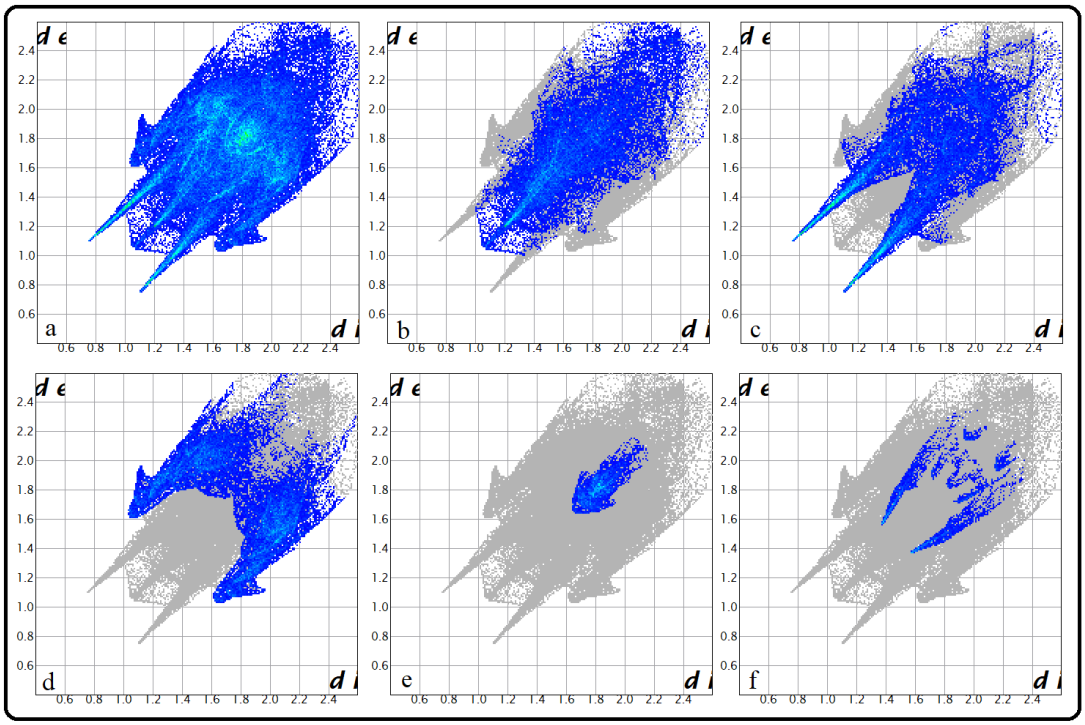

Şekil 7. The full two-dimensional fingerprint plots for the complex I, showing (a) all atoms interactions and delineated into (b) H···H, (c) H···O/O···H, (d) H···C/C···H, (e) C···C and (f) C···O/O···C interactions.

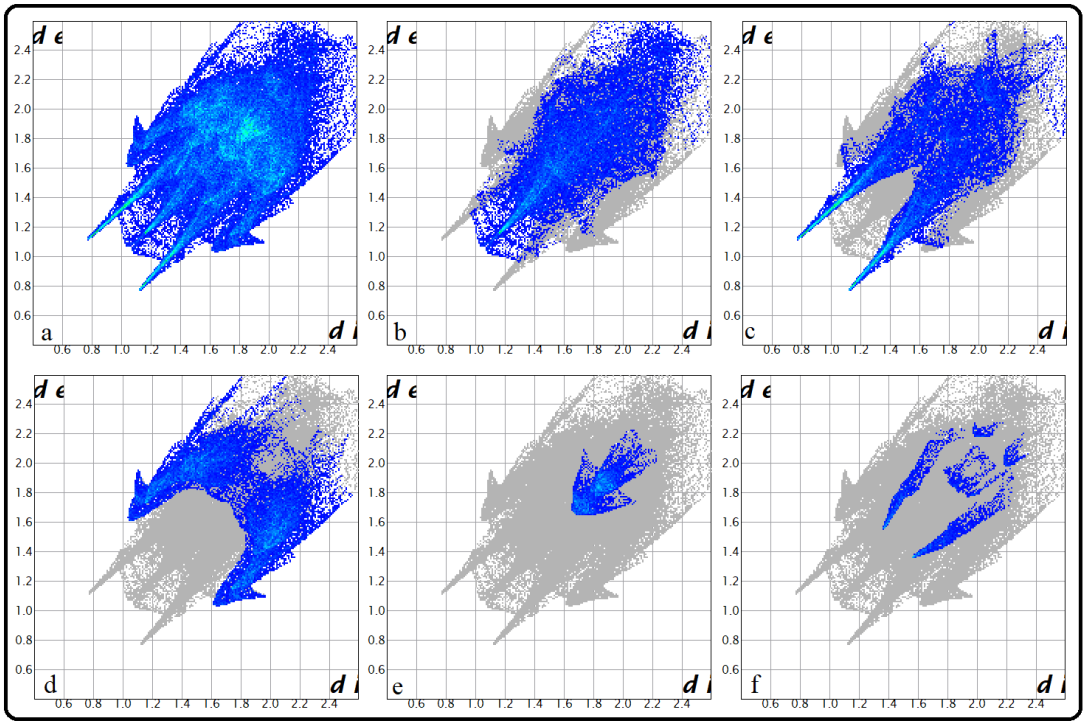

Şekil 8. The full two-dimensional fingerprint plots for the complex I, showing (a) all atoms interactions and delineated into (b) H···H, (c) H···O/O···H, (d) H···C/C···H, (e) C···C and (f) C···O/O···C interactions.

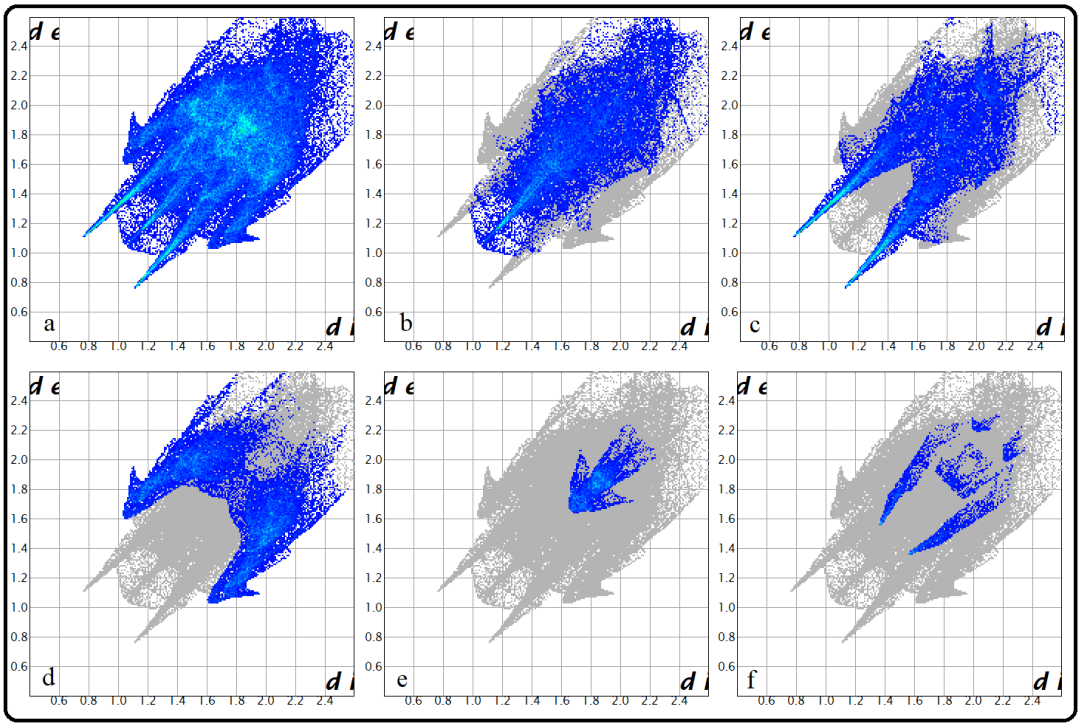

Şekil 9. The full two-dimensional fingerprint plots for the complex I, showing (a) all atoms interactions and delineated into (b) H···H, (c) H···O/O···H, (d) H···C/C···H, (e) C···C and (f) C···O/O···C interactions.

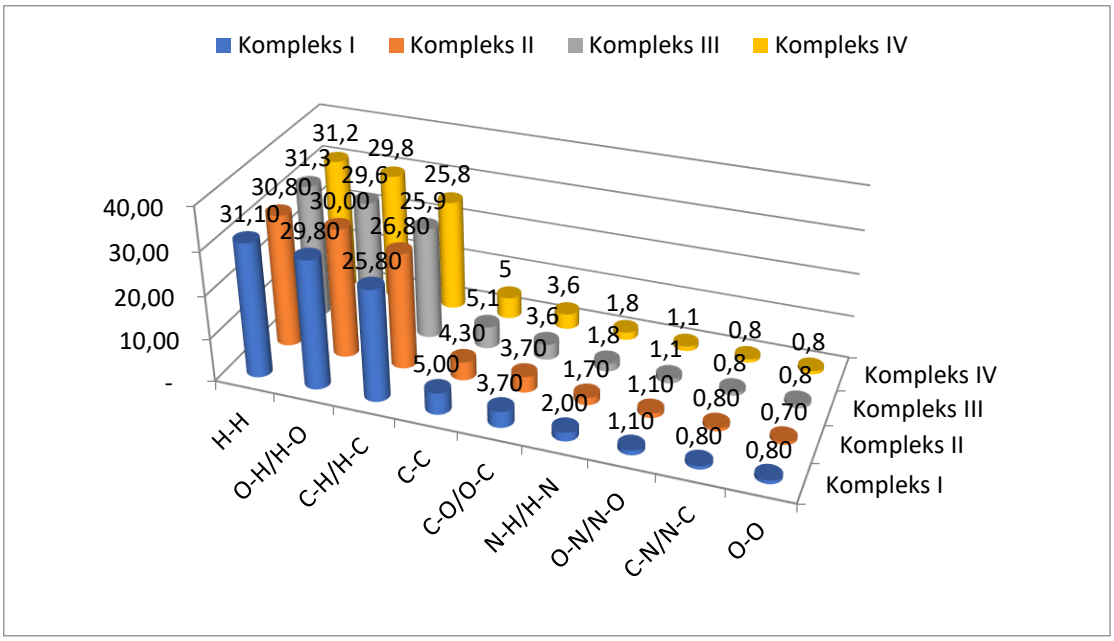

Figure 10. Molecular interaction percentages of all complex.

Interactions Energy Analysis

The interaction energies of the complex were calculated using CE-B3LYP/6-31G (d, p) and HF/3-21G in the Crystal Explorer program. In Figure 11-14, it is seen that the coulomb energy (a), dispersion energies (b) and total energy (c) are represented by energy frames. The computation of energy frames was developed to better understand the topology of the overall interaction energies between the components of a crystal. Total intermolecular interaction energy (E tot) using scale factors of 1.057, 0.740, 0.871 and 0.618, respectively, using four energy terms (electrostatic (E ele), polarization (E pol), dispersion (E disp) and exchange-repulsion (E rep)) are added together(Etse et al., 2020; Mackenzie et al., 2017; Madan Kumar, 2019). The closeness of the total energy values calculated in all four isostructural complexes is shown in Table 2. The very small differences that occur are not thought to be due to differences in the electronic configuration of metal atoms.

It has been determined that the energy values in different Cartesian coordinates are very close to each other. It has been determined that the electrostatic energy (E_ele) values significantly affect the total energy values. Studies have reported that hydrogen bond interactions contribute to electrostatic energy. In this structure, electrostatic energy is affected by the N-H…O and O-H…O hydrogen bonds and weak C-H…π interactions in the structure.

Table 1. Scale factors for benchmarked energy models (Mackenzie et al., 2017).

Energy Model	k_ele	k_pol	k_disp	k_rep
CE-HF ... HF/3-21G electron densities	1.019	0.651	0.901	0.811
CE-B3LYP ... B3LYP/6-31G(d,p) electron densities	1.057	0.740	0.871	0.618

Table 2. Interactions energy analysis results

	N	**Symop**	**R**	**Electron Density**	**E_ele**	**E_pol**	**E_dis**	**E_rep**	**E_tot**
I	2	x, y, z	7.78	B3LYP/6-31G(d,p)	-76.1	-20.5	-60.5	103.3	-84.6
	2	x, y, z	9.80	B3LYP/6-31G(d,p)	-6.7	-9.3	-59.7	37.2	-42.9
	2	x, y, z	14.41	B3LYP/6-31G(d,p)	-69.1	-19.3	-23.3	75.3	-61.1
	2	x, y, z	12.86	B3LYP/6-31G(d,p)	-34.8	-8.7	-53.1	48.3	-59.6
	2	x, y, z	9.90	B3LYP/6-31G(d,p)	-81.7	-34.0	-91.5	112.6	-121.7
					-268.4	-91.8	-288.1	-376.7	-369.9
	2	x, y, z	7.78	HF/3-21G	-92.9	-30.0	-60.5	76.1	-107.0
	2	x, y, z	9.80	HF/3-21G	-1.6	-10.4	-59.7	27.1	-40.2
	2	x, y, z	14.41	HF/3-21G	-62.8	-22.7	-23.3	54.8	-55.3
	2	x, y, z	12.86	HF/3-21G	-39.9	-12.0	-53.1	37.2	-66.1
	2	x, y, z	9.90	HF/3-21G	-87.2	-43.6	-91.5	88.7	-127.8
					-284.4	-118.7	-288.1	-283.9	-369.4
II	2	x, y, z	7.82	B3LYP/6-31G(d,p)	-66.6	-18.5	-59.4	91.9	-79.0
	2	x, y, z	9.65	B3LYP/6-31G(d,p)	-4.7	-9.2	-62.1	36.7	-43.3
	2	x, y, z	14.15	B3LYP/6-31G(d,p)	-74.3	-20.0	-23.6	81.3	-63.6
	2	x, y, z	12.71	B3LYP/6-31G(d,p)	-34.0	-8.1	-50.6	42.9	-59.5

	2	x, y, z	9.84	B3LYP/6-31G(d,p)	-80.8	-32.7	-89.6	109.2	-120.3
					260.4	-88.5	-285,3	-362	-365.7
	2	x, y, z	7.82	HF/3-21G	-82.0	-27.1	-59.4	65.9	-101.3
	2	x, y, z	9.65	HF/3-21G	-1.5	-10.1	-62.1	26.9	-39.1
	2	x, y, z	14.15	HF/3-21G	-69.0	-24.0	-23.6	59.4	-59.0
	2	x, y, z	12.71	HF/3-21G	-39.0	-11.2	-50.6	32.6	-66.2
	2	x, y, z	9.84	HF/3-21G	-82.0	-41.1	-89.6	80.3	-125.9
					-273.5	-113.5	-285.3	-261.1	-391.5
III	2	x, y, z	7.76	B3LYP/6-31G(d,p)	-72.6	-19.9	-61.5	105.0	-80.2
	2	x, y, z	9.82	B3LYP/6-31G(d,p)	-7.0	-9.6	-58.6	36.5	-43.0
	2	x, y, z	14.32	B3LYP/6-31G(d,p)	-68.4	-19.2	-23.6	74.4	-61.2
	2	x, y, z	12.87	B3LYP/6-31G(d,p)	-34.5	-8.8	-53.2	47.2	-60.1
	2	x, y, z	9.82	B3LYP/6-31G(d,p)	-84.9	-35.5	-91.4	113.2	-125.7
					-267.4	-93	-288.3	-376.3	-370.2
	2	x, y, z	7.76	HF/3-21G	-90.9	-29.6	-61.5	76.6	-105.2
	2	x, y, z	9.82	HF/3-21G	-1.4	-10.4	-58.6	26.5	-39.6
	2	x, y, z	14.32	HF/3-21G	-61.9	-22.5	-23.6	54.1	-55.1
	2	x, y, z	12.87	HF/3-21G	-39.2	-11.8	-53.2	36.4	-66.0
	2	x, y, z	9.82	HF/3-21G	-87.9	-43.9	-91.4	89.1	-128.2
					-281.3	-118.2	-288.3	-282.7	-394.1
IV	2	x, y, z	7.79	B3LYP/6-31G(d,p)	-75.5	-20.7	-60.3	98.6	-86.7
	2	x, y, z	9.79	B3LYP/6-31G(d,p)	-7.3	-9.5	-59.6	37.1	-43.7
	2	x, y, z	14.42	B3LYP/6-31G(d,p)	-69.5	-19.3	-23.4	75.2	-61.7

	2	x, y, z	12.85	B3LYP/6-31G(d,p)	-35.9	-8.9	-53.2	48.2	-61.1
	2	x, y, z	9.91	B3LYP/6-31G(d,p)	-82.1	-34.0	-91.4	112.2	-122.3
					-270.3	-92.4	-287.9	-371.3	375.5
	2	x, y, z	7.79	HF/3-21G	-91.8	-29.6	-60.3	72.6	-108.2
	2	x, y, z	9.79	HF/3-21G	-1.9	-10.4	-59.6	26.9	-40.6
	2	x, y, z	14.42	HF/3-21G	-62.7	-22.7	-23.4	54.6	-55.5
	2	x, y, z	12.85	HF/3-21G	-39.9	-12.0	-53.2	37.1	-66.3
	2	x, y, z	9.91	HF/3-21G	-87.0	-42.6	-91.4	88.1	-127.3
					-283.3	-117.3	-287.9	-279.3	397.9

E:interaction energies components, Symop: rotational symmetry operations with respect to the reference molecule, R: the centroid-to-centroid distance between the reference molecule N: interacting molecules as well as the number of pair(s) of interacting molecules with respect to the reference molecule (Mackenzie et al., 2017).

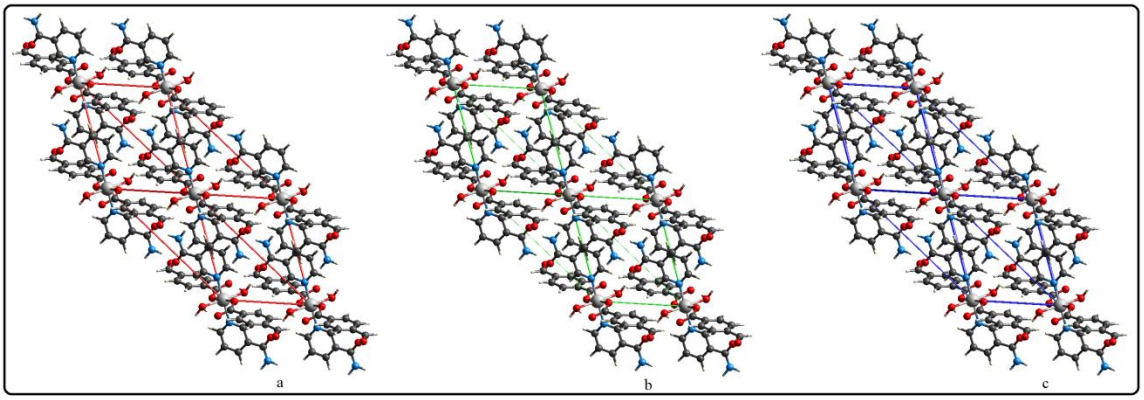

Figure 11. The energy framework showing coulomb energy (a) , dispersion energy (b) and total energy (c) diagrams.

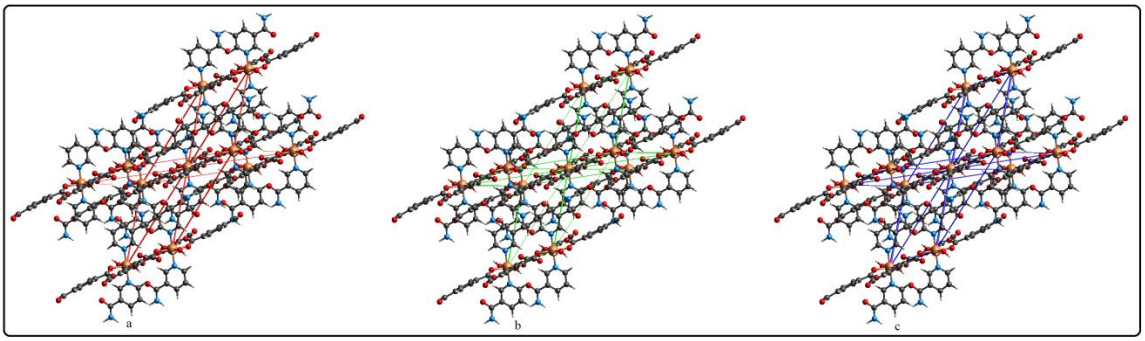

Figure 12. The energy framework showing coulomb energy (a) , dispersion energy (b) and total energy (c) diagrams.

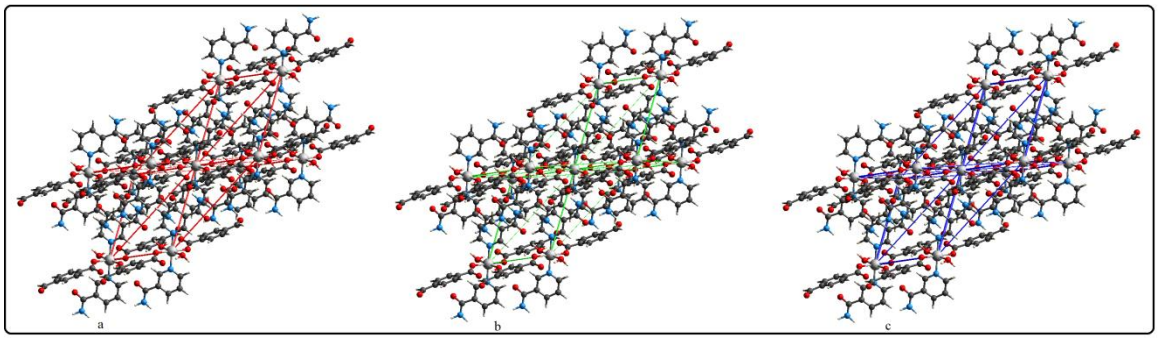

Figure 13. The energy framework showing coulomb energy (a) , dispersion energy (b) and total energy (c) diagrams.

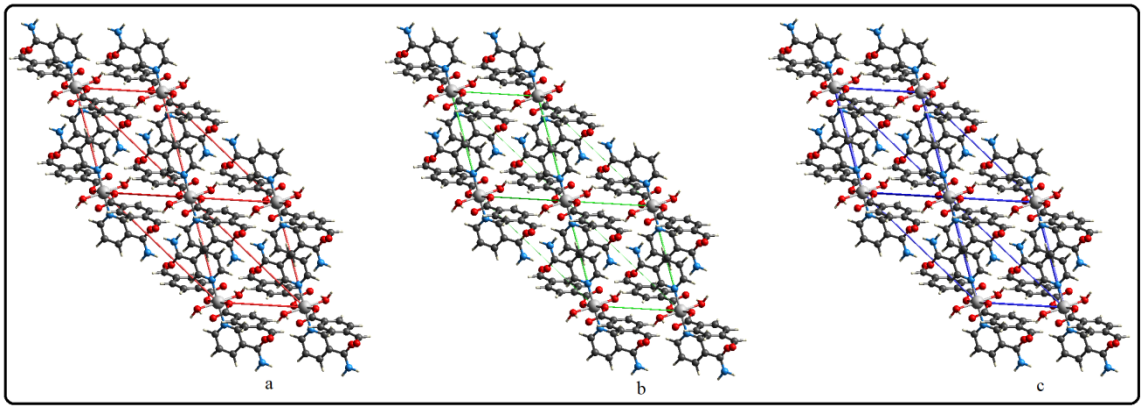

Figure 14. The energy framework showing coulomb energy (a) , dispersion energy (b) and total energy (c) diagrams.

CONCLUSION

In this study, the relationship between Hirshfeld surfaces of four complexes, metal(II) 4-formylbenzoate nicotinamide, 2D fingerprint plots and Interactions Energy Analysis was investigated. According to the results of hirshfield surface analysis in four isostructural complexes, the most dominant interactions in all complexes are H···H, O···H/H···O, C···H/H···C,

C···C, C···O/O···C, N···H/ H···N, O···N/N···O, C···N/N···C and O···O. Due to the presence of hydrogen bonds, the H···H, H···O/O···H and H···N/N···H interactions in the complex make an important contribution to the crystal packing of the complexes. The presence of adjacent red and blue triangles appearing in the shape index of the complexes supports the weak C-H…π and π-π stacking interactions between the benzene and pyridine rings in the crystal structures. Using two different models of CrystalExplorer (CE) software, polarization (E pol), dispersion (E dis) and change-repulsion (E rep) energies were calculated. The E_tot values calculated for isostructural complexes with the B3LYP/6-31G(d,p) energy model were found to be -369.9, -365.7, -370.2 and -375.5 kJ/mol, respectively. These values were also calculated for complexes by using the HF/3-21G energy model, and they were also found to be -369.4, -391.5, -394.1 and 397.9 kJ/mol, respectively. As a result, it is seen that the E_tot values of all complexes are very close to each other. Similar energy values were obtained due to the isostructure of the complexes.

Conflict of Interest

The author wish to declare that they have no conflict of interest

Authors contribution

The author did all the work himself.

REFERENCES

Etse, K. S., Lamela, L. C., Zaragoza, G., & Pirotte, B. (2020). Synthesis, crystal structure, Hirshfeld surface and interaction energies analysis of 5-methyl-1,3-bis(3-nitrobenzyl)pyrimidine-2,4(1H,3H)-dione. *European Journal of Chemistry*, *11*(2), Article 2. https://doi.org/10.5155/eurjchem.11.2.91-99.1973

Huseynova, M., Farzaliyev, V., Medjidov, A., Aliyeva, M., Taslimi, P., Sahin, O., & Yalçın, B. (2020). Novel zinc compound with thiosemicarbazone of glyoxylic acid: Synthesis, crystal structure, and bioactivity properties. *Journal of Molecular Structure*, *1200*, 127082. https://doi.org/10.1016/j.molstruc.2019.127082

Huseynova, M., Medjidov, A., Taslimi, P., & Aliyeva, M. (2019). Synthesis, characterization, crystal structure of the coordination polymer Zn (II) with thiosemicarbazone of glyoxalic acid and their inhibitory properties against some metabolic enzymes. *Bioorganic Chemistry*, *83*, 55–62. https://doi.org/10.1016/j.bioorg.2018.10.012

Huseynova, M. T. (2021). DFT calculations, hirshfeld analysis, antimicrobial, antifungal properties of the Cu(II) polymeric complex with thiosemicarbazone of glyoxylic acid. *Azerbaijan Chemical Journal*, *4*, 77–81. Scopus.

Irak, Z. T., & Beytur, M. (2019). 4-Benzilidenamino-4,5-dihidro-1H-1,2,4-triazol-5-on Türevlerinin Antioksidan Aktivitelerinin Teorik Olarak İncelenmesi. *Journal of the Institute of Science and Technology*, *9*(1), Article 1. https://doi.org/10.21597/jist.481990

Jayatilaka, D., Grimwood, D. J., Lee, A., Lemay, A., Russel, A. J., Taylor, C., Wolff, S. K., Cassam-Chenai, P., & Whitton, A. (2005). *TONTO - A System for Computational Chemistry. Available at: Http://hirshfeldsurface.net/*.

Kirste, B. (2016). *Applications of Density Functional Theory to Theoretical Organic Chemistry*. https://doi.org/10.4172/2150-3494.1000127

Koç, E., Yüksek, H., Beytur, M., Akyıldırım, O., Akçay, M., Beytur, C. (2020). In vivo determination of antioxidant property of heterocyclic 4,5 dihydro-1H-1, 2, 4- triazol 5-one derivate in male rats (wistar albino). *Bitlis Eren University Journal of Science, 9*, 542-548.

Kotan, G., Gökce, H., Akyıldırım, O., Yüksek, H., Beytur, M., Manap, S., & Medetalibeyoğlu, H. (2020). Synthesis, Spectroscopic and Computational Analysis of 2-[(2-Sulfanyl-1H-benzo[d]imidazol-5-yl)iminomethyl]phenyl Naphthalene-2-sulfonate. *Russian Journal of Organic Chemistry*, *56*(11), 1982–1994. https://doi.org/10.1134/S1070428020110135

Mackenzie, C. F., Spackman, P. R., Jayatilaka, D., & Spackman, M. A. (2017). CrystalExplorer model energies and energy frameworks: Extension to metal coordination compounds, organic salts, solvates and open-shell systems. *IUCrJ*, *4*(Pt 5), 575–587. https://doi.org/10.1107/S205225251700848X

Madan Kumar, S. (2019). 3D energy frameworks of dimethylbenzophenone tetramorphs. *Heliyon*, *5*(2), e01209. https://doi.org/10.1016/j.heliyon.2019.e01209

McKinnon, J. J., Jayatilaka, D., & Spackman, M. A. (2007). Towards quantitative analysis of intermolecular interactions with Hirshfeld surfaces. *Chemical Communications (Cambridge, England)*, *37*, 3814–3816.

Omoregie, H. O., Oloba-Whenu, O. A., Olowu, O. J., Fasina, T. M., Friedrich, A., Haehnel, M., & Marder, T. B. (2022). Mixed-ligand complexes of copper(II) with thienoyltrifluoroacetonate and nitrogen containing ligands: Synthesis, structures, antimicrobial activity, cytotoxicity, Hirshfeld surface analysis and DFT studies. *RSC Advances*, *12*(36), 23513–23526. https://doi.org/10.1039/D2RA02428D

Sertçelik, M. (2021). Synthesis, spectroscopic properties, crystal structures, DFT studies, and the antibacterial and enzyme inhibitory properties of a complex of Co(II) 3,5-difluorobenzoate with 3-pyridinol. *Journal of Chemical Research*, *45*(1–2), 42–48. https://doi.org/10.1177/1747519820924636

Sertçelik, M., Çaylak Delibaş, N., Çevik, S., Necefoğlu, H., & Hökelek, T. (2012). Poly[(μ5-2,2′-bipyridine-5,5′-dicarboxyl-ato)lead(II)]. *Acta Crystallographica Section E: Structure Reports Online*, *68*(9), Article 9. https://doi.org/10.1107/S1600536812035647

Sertçelik, M., Çaylak Delibaş, N., Necefoğlu, H., & Hökelek, T. (2012a). Diaqua-bis-(4-formyl-benzoato-κO1)bis-(nicotinamide-κN1)copper(II). *Acta Crystallographica Section E: Structure Reports Online*, *68*(7), Article 7. https://doi.org/10.1107/S1600536812028814

Sertçelik, M., Çaylak Delibaş, N., Necefoğlu, H., & Hökelek, T. (2012b). Diaqua-bis-(4-formyl-benzoato-κO1)bis-(nicotinamide-κN1)nickel(II). *Acta Crystallographica Section E: Structure Reports Online*, *68*(7), Article 7. https://doi.org/10.1107/S1600536812026943

Sertçelik, M., Çaylak Delibaş, N., Necefoğlu, H., & Hökelek, T. (2012c). Diaqua-bis-(4-formyl-benzoato-κO1)bis-(nicotinamide-κN1)cobalt(II). *Acta Crystallographica Section E: Structure Reports Online*, *68*(8), Article 8. https://doi.org/10.1107/S1600536812032205

Sertçelik, M., Çaylak Delibaş, N., Necefoğlu, H., & Hökelek, T. (2012d). Diaqua-bis-(4-formyl-benzoato-κO1)bis-(nicotinamide-κN1)zinc. *Acta Crystallographica Section E: Structure Reports Online*, *68*(8), Article 8. https://doi.org/10.1107/S160053681203320X

Sertcelik, M., & Durman, M. (2020). Synthesis, Characterization, and Antibacterial Activity of Cd(II) Complexes with 3-/4-Fluorobenzoates and 3-Hydroxypiridine as Co-Ligands. *Russian Journal of Inorganic Chemistry*, *65*(9), 1351–1359. https://doi.org/10.1134/S0036023620090168

Sertçelİk, M., Sugeçtİ, S., Büyükgüzel, E., Necefoğlu, H., & Büyükgüzel, K. (2018). Diaquabis N,N-dietilnikotinamid-lN1 bis 4-formilbenzoato-lO kobalt II Kompleksinin Model Organizma Galleria mellonella L. Lepidoptera: Pyralidae Üzerindeki Toksikolojik ve Fizyolojik Etkileri. *Karaelmas Fen ve Mühendislik Dergisi*, *8*(1), Article 1.

Spackman, M. A., & Jayatilaka, D. (2009). Hirshfeld surface analysis. *CrystEngComm*, *11*(1), 19–32. https://doi.org/10.1039/B818330A

Spackman, M. A., McKinnon, J. J., & Jayatilaka, D. (2008). Electrostatic potentials mapped on Hirshfeld surfaces provide direct insight into intermolecular interactions in crystals. *CrystEngComm*, *10*(4), 377–388. https://doi.org/10.1039/B715227B

Sugeçti, S., & Büyükgüzel, K. (2022). Effects of Ni (II) p-hydroxybenzoate with caffeine on metabolic, antioxidant, andbiochemical parameters of model insect Galleria mellonella L. (Lepidoptera: Pyralidae). *Turkish Journal of Zoology*, *46*(1), 167–174. https://doi.org/10.3906/zoo-2110-6

Turner, M. J., McKinnon, J. J., Wolff, S. K., Grimwood, D. J., Spackman, P. R., Jayatilaka, D., & Spackman, M. A. (2017). CrystalExplorer17. *University of Western Australia*.

Venkatesan, P., Thamotharan, S., Ilangovan, A., Liang, H., & Sundius, T. (2016). Crystal structure, Hirshfeld surfaces and DFT computation of NLO active (2E)-2-(ethoxycarbonyl)-3-[(1-methoxy-1-oxo-3-phenylpropan-2-yl)amino] prop-2-enoic acid. *Spectrochimica Acta Part A-Molecular and Biomolecular Spectroscopy*, *153*, 625–636. https://doi.org/10.1016/j.saa.2015.09.002